

Research Article

Flagellar Motility of *Trypanosoma cruzi* Epimastigotes

G. Ballesteros-Rodea,^{1,2,3} M. Santillán,⁴ S. Martínez-Calvillo,⁵ and R. Manning-Cela¹

¹Departamento de Biomedicina Molecular, Centro de Investigación y de Estudios Avanzados del IPN, 07000 México, DF, Mexico

²Facultad de Medicina Veterinaria y Zootecnia, UNAM, 04510 México, DF, Mexico

³Facultad de Ciencias Químicas, Universidad Autónoma Benito Juárez de Oaxaca, 68120 Oaxaca, Mexico

⁴Unidad Monterrey, Centro de Investigación y Estudios Avanzados del IPN, 66600 Monterrey, Mexico

⁵FES Iztacala, UBIMED, UNAM, Estado de México, 54090 México, DF, Mexico

Correspondence should be addressed to R. Manning-Cela, rmanning@cinvestav.mx

Received 15 July 2011; Revised 28 September 2011; Accepted 29 September 2011

Academic Editor: Abhay R. Satoskar

Copyright © 2012 G. Ballesteros-Rodea et al. This is an open access article distributed under the Creative Commons Attribution License, which permits unrestricted use, distribution, and reproduction in any medium, provided the original work is properly cited.

The hemoflagellate *Trypanosoma cruzi* is the causative agent of American trypanosomiasis. Despite the importance of motility in the parasite life cycle, little is known about *T. cruzi* motility, and there is no quantitative description of its flagellar beating. Using video microscopy and quantitative vectorial analysis of epimastigote trajectories, we find a forward parasite motility defined by tip-to-base symmetrical flagellar beats. This motion is occasionally interrupted by base-to-tip highly asymmetric beats, which represent the ciliary beat of trypanosomatid flagella. The switch between flagellar and ciliary beating facilitates the parasite's reorientation, which produces a large variability of movement and trajectories that results in different distance ranges traveled by the cells. An analysis of the distance, speed, and rotational angle indicates that epimastigote movement is not completely random, and the phenomenon is highly dependent on the parasite behavior and is characterized by directed and tumbling parasite motion as well as their combination, resulting in the alternation of rectilinear and intricate motility paths.

1. Introduction

Trypanosoma cruzi is a flagellated protozoan that is the causative agent of Chagas disease, a debilitating and incurable fatal illness that affects 20 million people in Latin America [1]. This parasite presents a complex, biphasic life cycle, moving between invertebrate and vertebrate hosts in which three alternate developmental forms (epimastigotes, metacyclic and bloodstream trypomastigotes, and amastigotes) can be identified by their morphological features. Amastigotes are characterized by the presence of a short flagellum, while epimastigotes and trypomastigotes have a long flagellum that emerges from the flagellar pocket, an organelle that together with the cytostome is involved in the endocytic and exocytic pathways of the parasite [2–5].

Like other flagellated cells, the flagellum of trypanosomatids propels the parasite through the action of its mechanochemical oscillator, which generates motile forces. Cilia and flagella are organelles that have been highly conserved over the course of evolution and are encountered

in a variety of organisms from protists to mammals. Therefore, the trypanosomatid flagellum shows the characteristic pattern of nine pairs of peripheral doublets and one central pair of axoneme microtubules that is conserved among eukaryotes. The peripheral microtubules bear inner and outer dynein arms, radial spokes, and nexin links, while the central-pair microtubules show specific projections. The doublets are tethered to the cell via the basal body and are attached to each other by nexin links. The dyneins are the molecular motors that cause adjacent microtubule doublets to slide past one another. The action of the dyneins is coordinated through a dynein-regulating complex, and the signals are transmitted across the radial spokes, which together produce the waveforms of cilia and flagella [6–8]. This sliding is translated into flagellar bending.

The flagella of trypanosomatids also present another structure that is unique to kinetoplastids, euglenoids, and dinoflagellates, which is named the paraflagellar rod (PFR) (reviewed in [9–11]). The PFR is a lattice-like structure that runs parallel to the axoneme within the flagellar membrane.

It has proximal, intermediate, and distal domains; its diameter is similar to that of the axoneme; it is anchored to the axoneme via connections to doublets 4 to 7 [12–14].

Because the flagellum is composed of diverse structures, and is highly dynamic, intense, and highly coordinated, conformational changes of the axonemal microtubules, associated structures and PFR are required to perform all of the functions in which the flagellum is involved. Reverse and forward genetic tools have been used to evaluate many aspects of flagellar function and movement. The main flagellar components have been silenced, disrupting flagellar motility. Thus, it has been shown in trypanosomes that the flagellum plays key roles in cell morphogenesis [15], attachment to the insect host epithelium [16], mitochondrial DNA segregation [17], and cell division [18]. In addition, flagellar motility has shown to be essential for *T. brucei* survival in the mammalian bloodstream [19].

Although the genetic approaches have allowed for a considerable increase in the knowledge of different aspects of flagellar function and movement, little is known about parasite motility modes and flagellar beat. Quantitative analyses of the flagellar beat in *T. brucei* [20, 21] and *L. major* [22] have been reported; however, there exists no description of flagellar beating in *T. cruzi*.

Recent structural analysis of the PFR during epimastigote flagellar beating in *T. cruzi* suggests that the three portions (proximal, intermediate, and distal) of the PFR are rearranged, undergoing dynamic remodeling during flagellar beating [5]. Nevertheless, a quantitative understanding of epimastigotes beating is still lacking, and very little is known about the motility of *T. cruzi* epimastigotes.

In the present study, we analyzed the motility and flagellar beating of *Trypanosoma cruzi* epimastigotes. Images of free-swimming epimastigotes were captured by video microscopy, and a quantitative analysis of the distance traveled by individual epimastigotes was performed. The time trajectory of each parasite was decomposed into distance, speed, and rotational angle to facilitate a more detailed quantitative vectorial analysis, and a population-wide analysis was also performed.

2. Materials and Methods

2.1. Parasites. Epimastigotes from the *T. cruzi* CL-Brenner strain (a well-characterized strain and a reference strain for the genome project) were cultured in liver infusion tryptose medium (LIT) containing 10% fetal bovine serum (FBS) and 0.1 mg/mL hemin at 28°C. For all experiments, the parasites were grown in homogeneous conditions and were sampled for use in experiments while in the logarithmic growth stage at 48 hours. The stock cultures were grown every 4 days using 1×10^6 parasites as an initial inoculum to guarantee the homogeneity and active motility of the parasites.

2.2. Video Microscopy and Motility Assays. The parasites were labeled with carboxy-fluorescein succinimidyl ester (CFSE) green fluorescent stain (Molecular Probes, Eugene, OR) as follows. Epimastigotes (5×10^6) in log-phase growth were

washed with 1X PBS and stained in 1 mL of PBS with 0.5 mM of CFSE at room temperature for 20 min in the dark. After three washes with 1X PBS, 10 μ L drops of epimastigotes (5×10^6 /mL of 1X PBS) were placed onto coverslips, and the parasites were allowed to move freely. The motility videos of the stained parasites were taken through an inverted confocal laser microscope (Leica SP5, DM 16000, Mo) with a 488 nm fluorescence excitation filter and an HCXPLAPO lambda blue 63x 1.4 NA oil objective. The images were captured and analyzed using the LAS AF software (*Leica Application Suite Advanced Fluorescence Lite*/1.7.0 build 1240 Leica Microsystems). The images were captured in the time series mode at a rate of 10 frames/sec and recorded at 10 sec/sample.

2.3. Image Processing and Statistical Treatment of Measurements. For motility assays, the movement of the labeled cells was measured and analyzed using the Image-Pro plus V 6.0 Media Cybernetics program. For trajectory analysis, we returned the datasets x_i and y_i , which represent the parasite horizontal and vertical coordinates, respectively, at time t_i , after the start of recording. The first step of the trajectory analysis was the calculation of the distance traveled between two consecutive times, t_i and t_{i+1} . For this calculation, we used the following well-known formula from vector analysis, which we implemented in *MATLAB 7.1*:

$$d_i = \sqrt{(x_{i+1} - x_i)^2 + (y_{i+1} - y_i)^2}. \quad (1)$$

Because all time intervals between consecutive points are 1 second long, each distance d_i is numerically equal to the corresponding velocity v_i . Once all instantaneous velocities v_i for a given parasite were obtained, the average individual parasite velocity \bar{v} and the corresponding velocity histograms were calculated. Next, the angles between two consecutive displacements $[t_{i-1}, t_i]$ and $[t_i, t_{i+1}]$ were calculated for each parasite using the following equation (also implemented in a custom *MATLAB 7.1* routine):

$$\theta_i = s_i \cos^{-1} \left(\frac{(x_{i+1} - x_i)(x_i - x_{i-1}) + (y_{i+1} - y_i)(y_i - y_{i-1})}{d_{i-1}d_i} \right), \quad (2)$$

where d_{i-1} and d_i are the distances traveled by the parasite during displacements $[t_{i-1}, t_i]$ and $[t_i, t_{i+1}]$, respectively, and s_i is given by

$$s_i = \frac{(x_i - x_{i-1})(y_{i+1} - y_i) - (y_i - y_{i-1})(x_{i+1} - x_i)}{|(x_i - x_{i-1})(y_{i+1} - y_i) - (y_i - y_{i-1})(x_{i+1} - x_i)|}. \quad (3)$$

From the theorems of vector analysis, it can be proven that $s_i = 1$ for a counter-clockwise rotation, while $s_i = -1$ otherwise. Once all angles θ_i were calculated for a parasite trajectory, we computed the corresponding histogram and repeated the procedure for all of the parasites studied. Because all histograms were approximately symmetrical, for each trajectory, we further calculated the average of the absolute value of the angle θ_i as a measure of the intricacy of the corresponding trajectory.

3. Results

3.1. Motility Analysis of Free-Swimming Epimastigotes. The motion of free-swimming epimastigotes was analyzed using video microscopy, and the videos were processed with the Image-Pro plus V 6.0 Media Cybernetics program to study the cells motility traces. Figure 1 illustrates the cell motility and flagellar beating of *T. cruzi* epimastigotes. The parasites were highly motile, and showed great variability of movements and trajectories, which was characterized by alternating periods of translational cell movement, tumble and shutdown (Figures 1(a), 1(b), and 1(c)) that resulted in different distance ranges traveled by the cells (Figure 1(d)). The main waveform was a tractile beat that initiated at the tip of the flagellum and propagated toward the base, resulting in forward cell propulsion. In the free-swimming epimastigotes in which cell motion was not impeded, the wave amplitude did not change detectably along the entire free flagellum (Figure 2), as observed in *Leishmania major* [22]. This tractile beat was occasionally interrupted for short periods of base-to-tip wave beats that led to the reorientation of the anterior flagellar end and then the parasite body with no evident backward motility (Figure 1(e) light blue region, Figure 3 and Video 1). These data suggest that *T. cruzi* shows a forward cell propulsion with a tip-to-base flagellar wave propagation, as has been reported for *Leishmania* and African trypanosomes [20, 22].

3.2. Free-Swimming Epimastigotes Travel Different Distance Ranges. Quantitative analysis of cell motility traces of the fluorescent epimastigote population showed that the average velocities of the parasites ranged from $1 \mu\text{m}/10 \text{ sec}$ to $400 \mu\text{m}/10 \text{ sec}$ (Figure 4). The highest percentage of parasites (30%) traveled at the maximum velocity ($400 \mu\text{m}/10 \text{ sec}$), while the next highest percentage of epimastigotes (21%) traveled at the minimum velocity ($1 \mu\text{m}/10 \text{ sec}$). The remaining epimastigotes traveled different distances at different speeds between these extremes (20% at $21\text{--}40 \mu\text{m}/10 \text{ sec}$, 14% at $41\text{--}60 \mu\text{m}/10 \text{ sec}$, 7% at $61\text{--}90 \mu\text{m}/10 \text{ sec}$, and 8% at $81\text{--}100 \mu\text{m}/10 \text{ sec}$) at variable levels without displaying a particular pattern. Even though the differences in the average velocities may have resulted from differences between cells in motion and cells attached to the microscope slide, all of the parasites had a vigorous motion, and the amplitude and frequency of the flagellar wave was constant.

3.3. Vectorial Analysis of Parasites Trajectories. The time trajectories of free-swimming epimastigotes through the liquid medium were decomposed into distance, speed, and rotational angle to facilitate a more detailed quantitative comparison. Vector analysis was then applied to characterize the speed and rotational angles of all individual trajectories of each parasite using a custom *MATLAB 7.1* routine, and the average behavior of the epimastigote population was determined.

The speed data showed that the speed of the parasites could be described by a Maxwell-Boltzmann distribution, suggesting that epimastigotes undergo Brownian-like

motion. The wide parasite-to-parasite variability in average speed ($v_i = 6.37 \pm 0.7$) suggests that, in addition to Brownian motion, flagellar beating also contributes to the motility of epimastigotes (Figure 5).

As shown in Figure 6, the rotational angle analysis indicated that the angular change was approximately symmetrical over the entire range from -180 to 180 degrees in the free-swimming parasites. This finding indicated that there is no preference in the direction toward which parasites rotate, and it suggests a high degree of stochasticity. As the rotational angle histograms were not flat but rather showed a different bias for each parasite, the movement of parasites was not completely random, and the phenomenon was highly dependent on parasite behavior. The smaller angles were produced during directional drift through directed motion, whereas the larger angles were produced during the spin and tumble stage when the flagellum does not show coherent directed motion. The rotational angle histogram for free-swimming parasite motion showed a peak centered at small angles, indicative of almost rectilinear paths, with few abrupt changes in direction. This behavior was clearly observed when speed and rotational angle were analyzed together (Figure 7). The same symmetrical behavior was observed in all the randomly chosen parasites analyzed, and the average angular change was $\theta_i = 85 \pm 15$, even for parasites that had traveled different distances.

Taken together, these results indicate that epimastigotes from the same population taken from the same cell culture and exposed to identical environmental conditions do not follow a single motility mode.

4. Discussion

Even though that the motility process of trypanosomatids is important for survival, completion of the life cycle, and establishment of parasite infection, the molecular mechanisms involved remain poorly understood.

The recent publication of complete genome sequences for *T. cruzi*, *T. brucei*, and *L. major* [23–25], the studies of the trypanosome flagellar proteome [19, 20], and the feasibility of genetic manipulability of these organisms have shed light on the key roles of some molecules that participate in parasite motility and flagellar function. However, little is currently known about the general characteristics of motility and the flagellum beating processes, and an in-depth quantitative description against which hypotheses could be tested is lacking. For the “Tritryps,” quantitative analyses of the flagellar beating and free-swimming motility properties have only been reported in *T. brucei* [20, 21] and *L. major* [22].

Using video microscopy and vectorial analysis of parasite trajectories, we have found that the motility of free-swimming epimastigotes of *T. cruzi* is characterized by (a) a large variability of movements and trajectories with alternating periods of translational movement, tumble, and shutdown of the parasites; (b) forward motility resulting from tip-to-base flagellar wave propagation; (c) a symmetrical rotational angle that indicates a high degree of stochasticity;

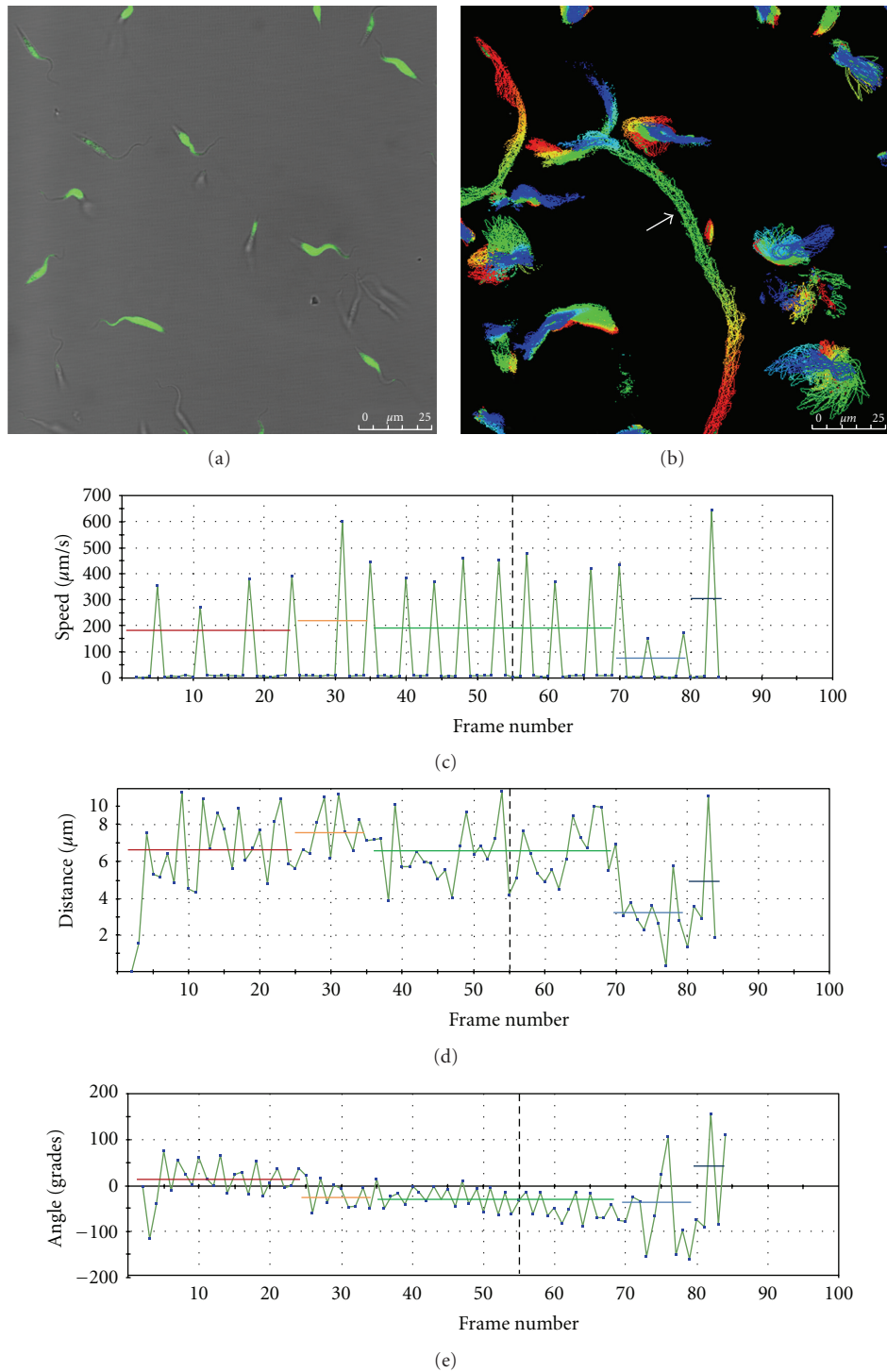


FIGURE 1: *Trypanosoma cruzi* motility analysis by time-lapse microscopy. (a) Direct observation of CFSE green fluorescent-labeled free-swimming epimastigotes analyzed by confocal microscopy. (b) Motility traces of epimastigotes. The positions of each individual cell are plotted at 10 frames/sec and recorded for 10 sec/sample. The starting position of each epimastigote is in red. The video clips used to generate these motility traces are available as supplementary material available at doi: 10.1155/2012/520380 (Video 1). The arrow indicates the parasite trajectory analyzed in panels (c, d, and e). The graphics represent the distance (c), angles (d), and speed (e) through consecutive frames of the selected parasite (arrow) of panel b. The color bars indicate the average value of each segment analyzed using the same color scale as the motility traces.

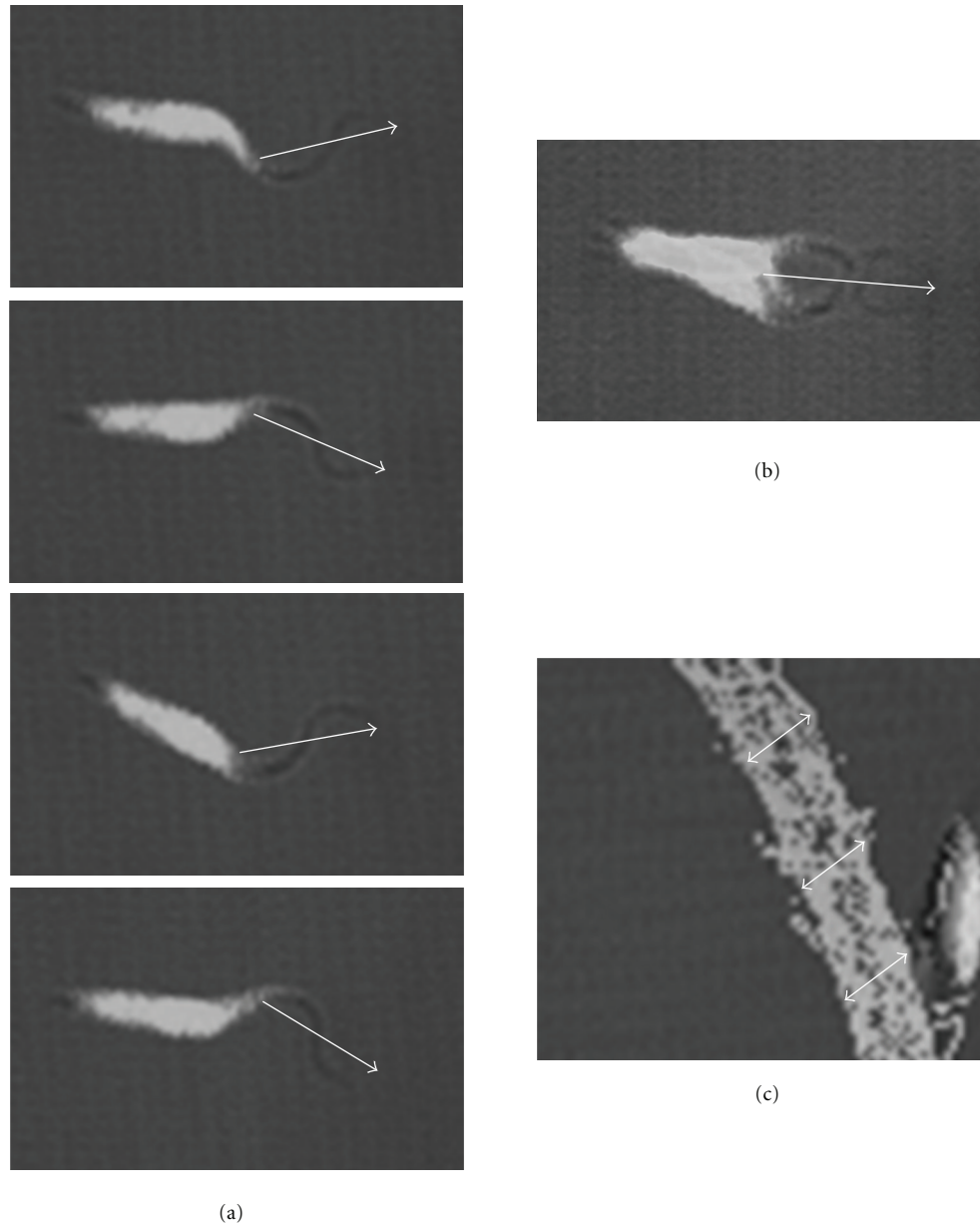


FIGURE 2: Analysis of the symmetrical flagellar beating of *T. cruzi*. (a) Parasite position and direction of motion (arrows) of four consecutive frames of an epimastigote with forward cell propulsion obtained from the green region of Figure 1. The amplitude and frequency of the flagellar wave were constant and symmetrical. (b) Fixed and superimposed images from panel a. (c) Plots of the movements and displacement of the epimastigote of panel (a). The arrows indicate the symmetry of parasite and flagellar wave contours during the cell displacement.

(d) flagellar beating that directs the epimastigote motility; (e) sporadic asymmetric base-to-tip beats that represent a ciliary beat of trypanosomatid flagella and produce a directional drift for the cell.

As for other trypanosomatids, the epimastigotes of *T. cruzi* swim very actively in any direction in the culture medium while leading with the anterior end. The parasite motility analysis presented in this work indicates that the cell traces have patterns similar to those previously reported for *T. brucei* [26, 27] and that the beating initiated from the flagellar tip is similar to that reported for *Leishmania* [22] and *T. brucei* [20]. This property of trypanosomatid flagella

is distinctive compared with most other organisms in which beating is initiated from the proximal end of the flagella. In these organisms, it was believed that bend formation and sustained regular oscillation depended upon a localized resistance to interdoublet sliding, which is usually conferred by structures at the flagellar base, known as the basal body. Similarly, in trypanosomes, it has been proposed that they may have some tip initiating or capping structure to provide resistance to doublet sliding in a manner similar to the basal body. This attachment structure has been found in *Crithidia deanei*, *Herpetomonas megaseliae*, *Trypanosoma brucei*, and *Leishmania major* [28]; therefore, this structure may also

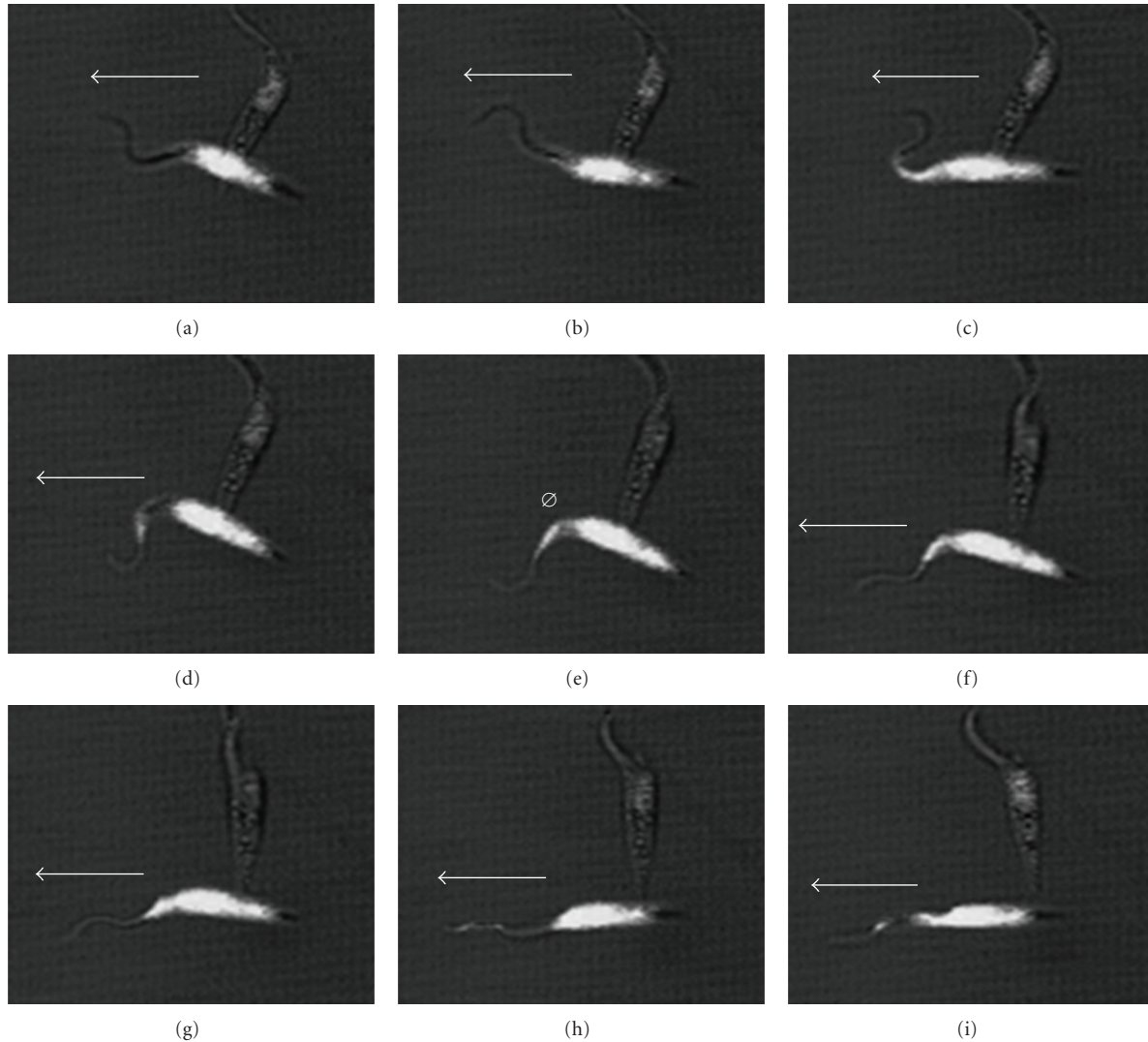


FIGURE 3: Illustration of the ciliary beat of *T. cruzi*. The forward parasite motility resulting from tip-to-base flagellar wave propagation (panels a–d) was interrupted by a sudden pause in which almost no movement of the parasite was observed (\emptyset). A base-to-tip wave propagation was observed before the parasite reinitiated the tip-to-base flagellar beat that resulted in a very little translational motion and clearly reoriented the parasite re-orientation and restarted the forward motion of the cell (panels f–i). These images correspond to those from an epimastigote obtained from the light blue region of Figure 1.

be present in *T. cruzi*, although future experiments will be needed to demonstrate this characteristic.

The beat initiation from points other than the flagellum tip, as reported for *L. major* and *T. brucei*, was difficult to evaluate in the *T. cruzi* epimastigotes because high-speed video microscopy was not used in this work. However, it was possible to detect that in addition to the tip-to-base flagellar wave, the epimastigotes also showed another type of beat that was propagated in the opposite direction (base-to-tip, which is characteristic of ciliary beating) at a much smaller frequency and in a highly asymmetric mode. This ciliary beat started spontaneously and interrupted the initiation of the main tip-to-base beat, producing a sudden pause in which almost no movement was observed. Then, a short interval of base-to-tip waves was noted before the

parasite reinitiated the tip-to-base flagellar beat that resulted in a very little translational motion and clearly produced a change in epimastigote orientation and the resumption of forward cell motion. This switch between flagellar and ciliary beating has been reported in *T. brucei* [20], *L. major*, *C. deanei*, *C. fasciculata* [22], and *C. oncopelti* [29]. These results indicate that these organisms are able to sustain at least two kinds of beat types and suggest that they are likely able to maintain other types of beats when are in different microenvironments during their life cycle.

The variability of movements and trajectories of *T. cruzi* epimastigotes is consistent with the tumbling, intermediate, and persistent motility modes observed in *T. brucei*. These motility modes are the result of the cell elongation that correlates with cell stiffness, which has been shown to affect

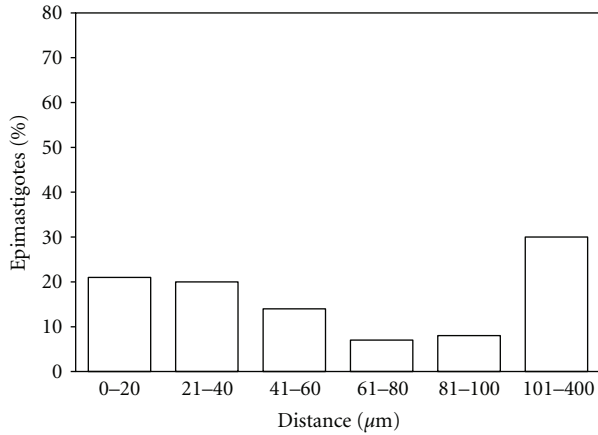


FIGURE 4: Quantitative motility analysis of free-swimming epimastigotes. The analysis of motility traces of fluorescent epimastigotes showed that the average velocities of the parasites ranged from 1 μm/10 second to 400 μm/10 sec. The histograms show the range of distances that each cell traversed per 10 sec. For each parasite trajectory, 100 randomly chosen cells were analyzed.

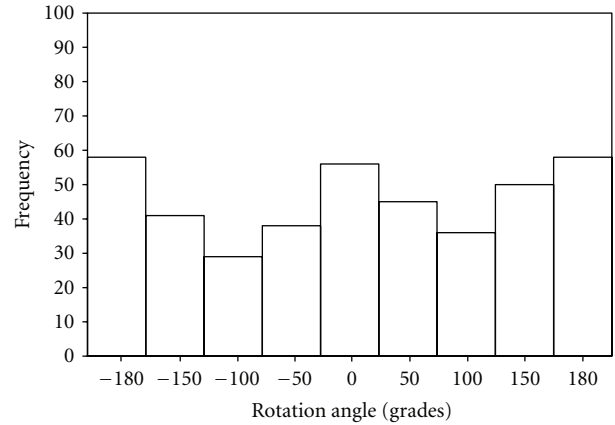


FIGURE 6: Analysis of flagellar rotational angle. The angles between two consecutive displacements were calculated for each parasite. The histogram is representative of the average behavior of 20 randomly selected epimastigotes.

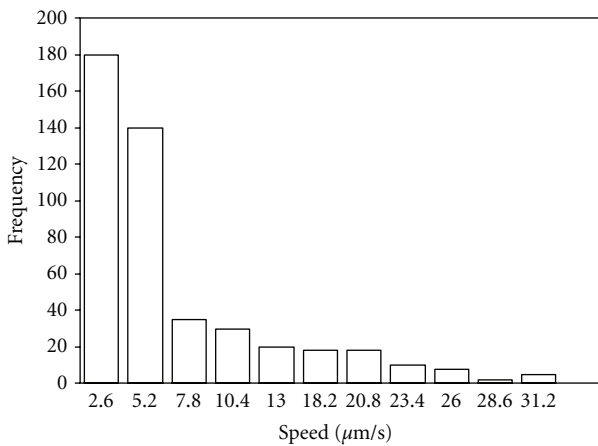


FIGURE 5: Analysis of cell speed. The speeds at which cells traveled through consecutive points during 1-sec time intervals were quantified in CFSE green fluorescent-labeled epimastigotes. The histogram is representative of the average behavior of 20 randomly selected epimastigotes.

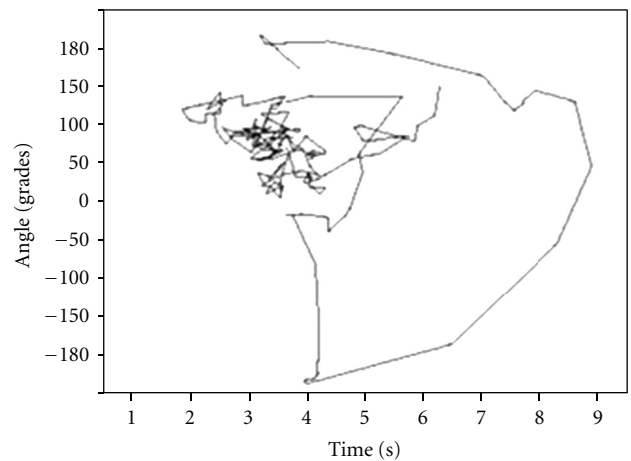


FIGURE 7: Analysis of parasite trajectory. The trajectory of free-swimming epimastigotes was determined using the speed and rotational angle results from a 10-second recording. The histogram is representative of the average behavior of 20 randomly selected epimastigotes.

not only flagellar velocities but also the directionality of parasite movement [21]. In *T. brucei* bloodstream forms, the flagellum runs along the cell body, resulting in complex body deformation during swimming, in which the straighter cells swim more directionally and cells that exhibit little net displacement appear to be more bent. Therefore, the predominance of directional motility in *T. cruzi* epimastigotes could have resulted from the higher amount of the straighter form of the cells, possibly because their flagellum runs along a short region of the cell body and because nonextensive parasite deformation is observed during cell swimming.

A recent analysis of the structural organization of the PFR of *T. cruzi* epimastigotes in flagella in straight versus

bent states [5] suggests that the PFR changes according to the movement of the axoneme. The PFR is composed of discrete filaments structured in lattice-like arrays with three distinct domains (proximal, intermediate, and distal), and it has been proposed that the three domains may work together. According to this proposal, when the proximal domain is compressed, the distal or opposite domain is stretched in an alternating pattern during flagellar beating. The intermediate domain would follow this dynamic of movement, and in a bent state, the filaments would get closer [5]. Therefore, the different motility modes observed during the swimming of epimastigotes could be an indication that the intermediate domain is able to change its position between the proximal

and distal filaments, allowing the switch between flagellar and ciliary beating. The movement of this domain would alternate the periods of translational cell movement, tumble, and shutdown of the parasite and result in the consequent reorientation of the epimastigotes. The mechanism by which the different modes of motility are coordinated is still unknown, but the minor components of the PFR [30] could participate as motor, anchoring, or connector proteins in the different modes of movement. However, future biochemical and genetic studies will be necessary to determine the type, function, and possible participation in the flagellar beat of these proteins.

The symmetry and equal amplitude waves through the flagellum observed in the directional motility of *T. cruzi* epimastigotes closely resemble that reported for promastigotes of *L. major*, which also has a free flagellum that is only attached along a short region of the cell body [22, 31]. Quantitative analysis of the rotational angle and study of separated parasite displacement and flagellar beating, using the corresponding fixed and superimposed images, revealed that, as in *Leishmania*, *T. cruzi* did not show changes in amplitude as the wave travelled from tip to base. In contrast, in *T. brucei*, the amplitude was reduced toward the proximal end, possibly due to the attachment of its flagellum along most of the cell body [20]. To test this hypothesis, future experiments comparing the flagellar beating of epimastigotes versus bloodstream and metacyclic trypomastigotes of *T. cruzi* will be useful.

The trypanosomatid flagellum is completely different from rotary-motor based bacterial flagella [32] and more complex than most other microtubule-based eukaryotic flagella [33, 34]. *T. cruzi*, like the other two “Tritryps” whose genome sequences have been determined, can be genetically manipulated for functional studies, is easily grown and transformed in culture, and its motility is an important part of its life cycle. For these reasons, the “Trityps” are becoming very attractive models for the analysis of flagellar function and the study of genes involved in human genetic disorders linked to flagellar motility defects. Therefore, the quantitative description of motility and flagellar beating of *T. cruzi* reported in this work provides a useful platform for future genetic experiments to test parasite motility and flagellar function hypotheses.

In summary, our quantitative motility analysis results offer insights into flagellar beating of the American trypanosome and provide new detail on an important, yet poorly understood, motility mode of *T. cruzi*.

Acknowledgments

This work was supported by CONACYT Grants nos. 42862 and 60152 awarded to R. G. Manning-Cela, Grant no. 55228 awarded to M. Santillán, and by Grants no. 128461 from CONACyT and no. IN203909 from PAPIIT (UNAM) awarded to S. Martínez-Calvillo. G. Ballesteros-Rodea received a doctoral scholarship from CONACYT (México). We thank Ivan Galván for guidance during the confocal microscopy analysis.

References

- [1] M. P. Barrett, R. J. Burchmore, A. Stich et al., “The trypanosomiasis,” *The Lancet*, vol. 362, no. 9394, pp. 1469–1480, 2003.
- [2] W. De Souza, “Basic cell biology of *Trypanosoma cruzi*,” *Current Pharmaceutical Design*, vol. 8, no. 4, pp. 269–285, 2002.
- [3] K. Gull, “Host-parasite interactions and trypanosome morphogenesis: a flagellar pocketful of goodies,” *Current Opinion in Microbiology*, vol. 6, no. 4, pp. 365–370, 2003.
- [4] I. Porto-Carreiro, M. Attias, K. Miranda, W. De Souza, and N. Cunha-E-Silva, “*Trypanosoma cruzi* epimastigote endocytic pathway: cargo enters the cytostome and passes through an early endosomal network before storage in reservosomes,” *European Journal of Cell Biology*, vol. 79, no. 11, pp. 858–869, 2000.
- [5] G. M. Rocha, S. H. Seabra, K. R. de Miranda, N. Cunha-e-Silva, T. M. de Carvalho, and W. de Souza, “Attachment of flagellum to the cell body is important to the kinetics of transferrin uptake by *Trypanosoma cruzi*,” *Parasitology International*, vol. 59, no. 4, pp. 629–633, 2010.
- [6] C. J. Brokaw, “Flagellar movement: a sliding filament model,” *Science*, vol. 178, no. 4060, pp. 455–462, 1972.
- [7] G. Piperno, K. Mead, and W. Shestak, “The inner dynein arms I2 interact with a “dynein regulatory complex” in *Chlamydomonas flagella*,” *Journal of Cell Biology*, vol. 118, no. 6, pp. 1455–1463, 1992.
- [8] E. F. Smith and W. S. Sale, “Regulation of dynein-driven microtubule sliding by the radial spokes in flagella,” *Science*, vol. 257, no. 5076, pp. 1557–1559, 1992.
- [9] P. Bastin, T. Sherwin, and K. Gull, “Paraflagellar rod is vital for trypanosome motility,” *Nature*, vol. 391, no. 6667, p. 548, 1998.
- [10] K. S. Ralston and K. L. Hill, “The flagellum of *Trypanosoma brucei*: new tricks from an old dog,” *International Journal for Parasitology*, vol. 38, no. 8–9, pp. 869–884, 2008.
- [11] J. A. Maga and J. H. LeBowitz, “Unravelling the kinetoplastid paraflagellar rod,” *Trends in Cell Biology*, vol. 9, no. 10, pp. 409–413, 1999.
- [12] M. H. Abdille, S. Y. Li, Y. Jia, X. Suo, and G. Mkoji, “Evidence for the existence of paraflagellar rod protein 2 (PFR2) gene in *Trypanosoma evansi* and its conservation among other kinetoplastid parasites,” *Experimental Parasitology*, vol. 118, no. 4, pp. 614–618, 2008.
- [13] F. Rusconi, M. Durand-Dubief, and P. Bastin, “Functional complementation of RNA interference mutants in trypanosomes,” *BMC Biotechnology*, vol. 5, article 6, 2005.
- [14] T. Souto-Padron, T. U. de Carvalho, E. Chiari, and W. de Souza, “Further studies on the cell surface charge of *Trypanosoma cruzi*,” *Acta Tropica*, vol. 41, no. 3, pp. 215–225, 1984.
- [15] L. Kohl, D. Robinson, and P. Bastin, “Novel roles for the flagellum in cell morphogenesis and cytokinesis of trypanosomes,” *The Embo Journal*, vol. 22, no. 20, pp. 5336–5346, 2003.
- [16] L. Tetley and K. Vickerman, “Differentiation in *Trypanosoma brucei*: host-parasite cell junctions and their persistence during acquisition of the variable antigen coat,” *Journal of Cell Science*, vol. 74, pp. 1–19, 1985.
- [17] D. R. Robinson and K. Gull, “Basal body movements as a mechanism for mitochondrial genome segregation in the trypanosome cell cycle,” *Nature*, vol. 352, no. 6337, pp. 731–733, 1991.

- [18] F. F. Moreira-Leite, T. Sherwin, L. Kohl, and K. Gull, "A trypanosome structure involved in transmitting cytoplasmic information during cell division," *Science*, vol. 294, no. 5542, pp. 610–612, 2001.
- [19] R. Broadhead, H. R. Dawe, H. Farr et al., "Flagellar motility is required for the viability of the bloodstream trypanosome," *Nature*, vol. 440, no. 7081, pp. 224–227, 2006.
- [20] C. Branche, L. Kohl, G. Toutirais, J. Buisson, J. Cosson, and P. Bastin, "Conserved and specific functions of axoneme components in trypanosome motility," *Journal of Cell Science*, vol. 119, no. 16, pp. 3443–3455, 2006.
- [21] S. Uppaluri, J. Nagler, E. Stellamanns et al., "Impact of microscopic motility on the swimming behavior of parasites: straighter Trypanosomes are more directional," *Plos Computational Biology*, vol. 7, no. 6, Article ID e1002058, 2011.
- [22] C. Gadelha, B. Wickstead, and K. Gull, "Flagellar and ciliary beating in trypanosome motility," *Cell Motility and the Cytoskeleton*, vol. 64, no. 8, pp. 629–643, 2007.
- [23] M. Berriman, E. Ghedin, C. Hertz-Fowler et al., "The genome of the African trypanosome *Trypanosoma brucei*," *Science*, vol. 309, no. 5733, pp. 416–422, 2005.
- [24] N. M. El-Sayed, P. J. Myler, G. Blandin et al., "Comparative genomics of trypanosomatid parasitic protozoa," *Science*, vol. 309, no. 5733, pp. 404–435, 2005.
- [25] A. C. Ivens, C. S. Peacock, E. A. Worthey et al., "The genome of the kinetoplastid parasite, *Leishmania major*," *Science*, vol. 309, no. 5733, pp. 436–442, 2005.
- [26] P. Bastin, T. J. Pullen, T. Sherwin, and K. Gull, "Protein transport and flagellum assembly dynamics revealed by analysis of the paralysed trypanosome mutant *sln-1*," *Journal of Cell Science*, vol. 112, no. 21, pp. 3769–3777, 1999.
- [27] N. R. Hutchings, J. E. Donelson, and K. L. Hill, "Trypanin is a cytoskeletal linker protein and is required for cell motility in African trypanosomes," *Journal of Cell Biology*, vol. 156, no. 5, pp. 867–877, 2002.
- [28] D. Woolley, C. Gadelha, and K. Gull, "Evidence for a sliding-resistance at the tip of the trypanosome flagellum," *Cell Motility and the Cytoskeleton*, vol. 63, no. 12, pp. 741–746, 2006.
- [29] M. E. Holwill and J. L. McGregor, "Effects of calcium on flagellar movement in the trypanosome *Crithidia oncopelti*," *Journal of Experimental Biology*, vol. 65, no. 1, pp. 229–242, 1976.
- [30] F. F. Moreira-Leite, W. de Souza, and N. L. da Cunha-d-Silva, "Purification of the paraflagellar rod of the trypanosomatid *Herpetomonas megaseliae* and identification of some of its minor components," *Molecular and Biochemical Parasitology*, vol. 104, no. 1, pp. 131–140, 1999.
- [31] W. Souza, "Structural organization of *Trypanosoma cruzi*," *Memorias do Instituto Oswaldo Cruz*, vol. 104, supplement 1, pp. 89–100, 2009.
- [32] F. A. Samatey, K. Imada, S. Nagashima et al., "Structure of the bacterial flagellar protofilament and implications for a switch for supercoiling," *Nature*, vol. 410, no. 6826, pp. 331–337, 2001.
- [33] U. W. Goodenough and J. E. Heuser, "Substructure of inner dynein arms, radial spokes, and the central pair/projection complex of cilia and flagella," *Journal of Cell Biology*, vol. 100, no. 6, pp. 2008–2018, 1985.
- [34] D. Nicastro, C. Schwartz, J. Pierson, R. Gaudette, M. E. Porter, and J. R. McIntosh, "The molecular architecture of axonemes revealed by cryoelectron tomography," *Science*, vol. 313, no. 5789, pp. 944–948, 2006.